Journal of Applied Polymer Science

Thermal properties and degradation behavior of poly(1,4-butylene adipate)/modified layered double hydroxide nanocomposites

Mei-Chen Chu, Yi-Tong Hang, Yi-An Chen, Tzong-Ming Wu
Department of Materials Science and Engineering, National Chung Hsing University, 250 Kuo Kuang Road, Taichung 402, Taiwan
Correspondence to: T.-M. Wu (E-mail: tmwu@dragon.nchu.edu.tw)

ABSTRACT: In this study, poly(1,4-butylene adipate) (PBA)/organomodified layered double hydroxide (m-LDH) nanocomposites were synthesized and characterized as a new material for green materials use. m-LDH was initially prepared with magnesium nitrate hexahydrate, aluminum nitrate-9-hydrate, oleic acid, and sorbitol by a novel one-step coprecipitation method to intercalate the oleic acid and sorbitol organomodifier into the interlayer of the layered double hydroxide. The solution mixing process was then applied and shown to be an efficient method for fabricating the PBA/m-LDH nanocomposites. The m-LDH characterized by X-ray diffraction (XRD) showed a high interlayer spacing of 58.8 Å. The morphology and thermal properties of the PBA/m-LDH nanocomposites were characterized with XRD, transmission electron microscopy, and thermogravimetric analysis. It was shown that the m-LDH was well distributed in the PBA matrix and that the thermal properties of the PBA/m-LDH nanocomposites significantly improved with a loading of 0.1 wt % m-LDH. Finally, the biodegradability of the PBA/m-LDH nanocomposites was tested with lipase from *Pseudomonas fluorescens* as a microbial catalyst. It was shown that an addition of m-LDH up to 0.5% resulted in a significant difference in terms of the biodegradability. After 120 h of degradation, the residual weight and surface morphology of the composite films were affected by the presence of m-LDH. © 2015 Wiley Periodicals, Inc. J. Appl. Polym. Sci. **2015**, *132*, 42083.

KEYWORDS: biodegradable; composites; degradation; thermal properties

Received 2 October 2014; accepted 9 February 2015
DOI: 10.1002/app.42083

INTRODUCTION

In the past century, the extensive applications of synthetic polymers and their downstream products have become great additions to our daily lives. However, the polymers contain exceptional environmental stability, and their poor degradability will have apparent ecological effects. Therefore, several biocompatible and biodegradable polymers, including poly(1,4-butylene adipate) (PBA), polyhydroxyalkanoate, and poly(lactic acid), obtained from renewable materials have been widely used as acceptable substitutes for traditional petroleum-derived plastics.[1,2] PBA is a synthetic aliphatic polyester, which contains α- or β-form crystal with various crystallization temperatures.[3,4] The α-form crystal is thermodynamically stable because its equilibrium melting temperature is higher than that of the β-form crystal.[5] However, the practical applications of PBA are limited because of its slow crystallization rate, low thermal stability, and softness. The ability to solve the abovementioned problems in a convenient and effective method is of extensive interest.[6] In general, the addition of inorganic fillers to the polymer matrix as reinforcement materials can enhance the polymer's hardness, thermal properties, and crystallization rate.

Reinforcing materials of numerous sizes and shapes have been well used in polymer composites.[7] Nevertheless, the effect of reinforcing materials on the degradation behaviors of PBA composites have rarely been mentioned in these reports. Layered double hydroxides (LDHs) belong to a class of synthetic two-dimensional inorganic materials with lamellar structures.[8] Compared to two-dimensional montmorillonite, LDHs retain strong electrostatic interactions and a high charge density between hydroxide layers; this makes the delamination of LDHs within the polymer matrix more challenging.[9] One resolution is to expand the interlayer distance of LDH platelets with organomodifiers; this would also modify the surface properties of the LDHs from the hydrophilic attributes into hydrophobic ones.[10–13] Even though various organomodifiers have been effectively used as intercalation compounds of LDH, most of them are not biocompatible and may not appropriate for use in food-packaging materials and biomedical applications.

In this study, we proposed an approach for fabricating biodegradable PBA/organomodified layered double hydroxide (m-LDH) nanocomposites with a solution mixing process. m-LDH was prepared with biocompatible oleic acid and sorbitol

as an organomodifier through a one-step coprecipitation method. The structure, morphology, and thermal properties of the PBA/m-LDH nanocomposites were characterized with X-ray diffraction (XRD), transmission electron microscopy (TEM), and thermogravimetric analysis (TGA). The biodegradability of the PBA/m-LDH nanocomposite was investigated with lipase from *Pseudomonas fluorescens*.

EXPERIMENTAL

Materials

Sorbitol and lipase from *P. fluorescens* were purchased from Sigma-Aldrich Chemical Co. Magnesium nitrate hexahydrate [$Mg(NO_3)_2 \cdot 6H_2O$], aluminum nitrate-9-hydrate [$Al(NO_3)_3 \cdot 9H_2O$], and sodium hydroxide (NaOH) were obtained from Fluka Chemical Co. Chloroform and oleic acid were purchased from Mallinckrodt Baker and Showa, respectively. All of the chemicals were used without further purification.

PBA, purchased from Sigma-Aldrich Chemical Co., was purified by it mixture in a chloroform solution followed by precipitation at −10°C. The purified PBA was filtered and then vacuum-dried at 40°C for 72 h. m-LDHs with an Mg/Al molar ratio of 2 were synthesized by the one-step coprecipitation method with biocompatible oleic acid and sorbitol as an organomodifier. The reactants of 0.02 mol of $Mg(NO_3)_2 \cdot 6H_2O$ and 0.01 mol of $Al(NO_3)_3 \cdot 9H_2O$ were dissolved in 50 mL of deionized water at room temperature. The organomodifiers, 0.012 mol of oleic acid and 0.012 mol of sorbitol, were individually dissolved in the 100 mL of deionized water. Then, an aqueous solution containing the reactants $Mg(NO_3)_2 \cdot 6H_2O$, $Al(NO_3)_3 \cdot 9H_2O$, oleic acid, and sorbitol was vigorously stirred at 90°C for 24 h; the pH value was simultaneously maintained at 10.0 ± 0.2 by the dropwise addition of a 2*N* NaOH solution. All of the experimental processes were carried on under a nitrogen atmosphere. The obtained precipitates were filtered and washed systematically three times with ethanol, after which the remaining solids of LDH were freeze-dried and stored before further use. For comparison, LDH prepared with the same coprecipitation method without oleic acid and sorbitol was obtained.

Preparation of the PBA/m-LDH Nanocomposites

Various concentrations of PBA/m-LDH solution were prepared by a solution mixing process in chloroform. An amount of 0.1 g of PBA was dissolved in 10 mL of chloroform and mechanically stirred for 24 h. Simultaneously, different weight ratios (0.1, 0.2, and 0.5 wt %) of m-LDH were added to 10 mL of chloroform and ultrasonicated for 24 h to form a stable dispersion. The PBA/m-LDH nanocomposites were prepared by a solution-direct intercalation process in a chloroform solution and mechanically stirred for 6 h. The obtained solutions were poured into a glass Petri dish and dried *in vacuo* at 40°C for 24 h. All of the fabricated PBA/m-LDH nanocomposites contained α-form crystals.

Characterization of the PBA/m-LDH Nanocomposites

A wide-angle XRD experiment with Ni-filtered Cu Kα radiation was recorded on a Bruker D8 Discover instrument. Fourier transform infrared (FTIR) measurements were recorded on a PerkinElmer Spectrum One spectrometer in transmission mode from 400 to 4000 cm^{-1} with an average of 30 spectra recorded per sample. TEM, performed on a Hitachi HF-2000 at 200 kV, was used to characterize the distribution of m-LDH within the PBA/m-LDH nanocomposites. To observe the stacked LDH within the polymer matrix, the sample was immobilized in epoxy resin. Then, the resin embedded samples were microtomed at room temperature with a Reichert Ultracut ultramicrotome equipped with a diamond knife. The slices were collected on carbon-coated copper grids. TEM analysis was obtained with a sample of the carbon-coated copper grid. The thermal degradation behaviors of the PBA/m-LDH nanocomposites were carried out with a PerkinElmer TG/DTA 6300 thermoanalyzer. All of the samples were examined from room temperature to 600°C under a nitrogen atmosphere at a heating rate of 10°C/min. The biodegradability of the PBA/m-LDH nanocomposites was tested by microbial degradation with lipase from *P. fluorescens*. All of the chloroform-cast film samples were sterilized by UV radiation for 15 min before the microbial degradation test. Samplings were done at degradation times of 0, 24, 48, 72, 96, and 120 h for the measurement of residual weight and field-emission scanning electron microscopy (FESEM). The percentage of weight loss was calculated from $[100(W_0 - W_t)]/W_0$, where W_0 is the initial weight and W_t is the weight after biodegradation. FESEM was performed at 3 kV with a JEOL JSM-6700F field-emission instrument.

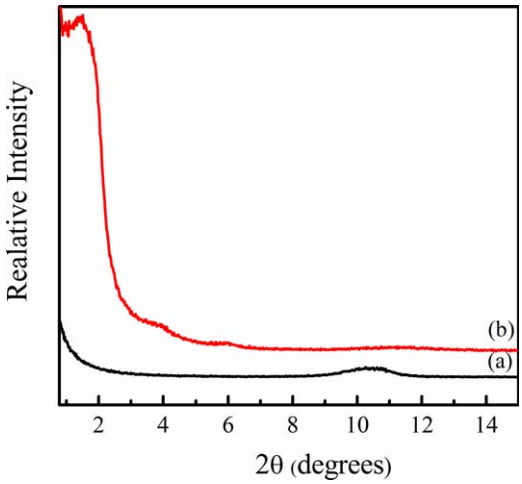

Figure 1. XRD data for (a) LDH and (b) m-LDH. [Color figure can be viewed in the online issue, which is available at wileyonlinelibrary.com.]

RESULTS AND DISCUSSION

Characterization of the Prepared m-LDH

The structures of LDH and m-LDH synthesized by the coprecipitation method were identified by XRD patterns, as shown in Figure 1. From the XRD data of LDH, there was a strong diffraction peak at $2\theta = 10.6°$; this corresponded to an interlayer distance of the (003) plane.[14,15] According to Bragg's equation, the interlayer spacing of LDH was equal to 8.3 Å. For the m-LDH, the XRD diffraction peak shifted to a smaller angle ($2\theta = 1.4°$); this revealed that the interlayer spacing of the LDH increased surprisingly to 58.8 Å with the addition of oleic acid and sorbitol. The molecular sizes of oleic acid and sorbitol were roughly estimated with Materials Studio software to be about

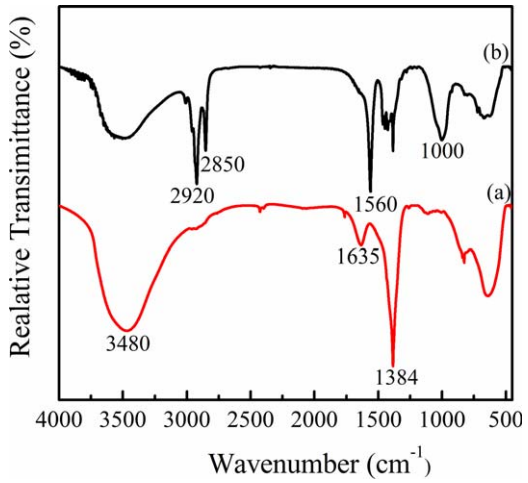

Figure 2. FTIR spectra of (a) LDH and (b) m-LDH. [Color figure can be viewed in the online issue, which is available at wileyonlinelibrary.com.]

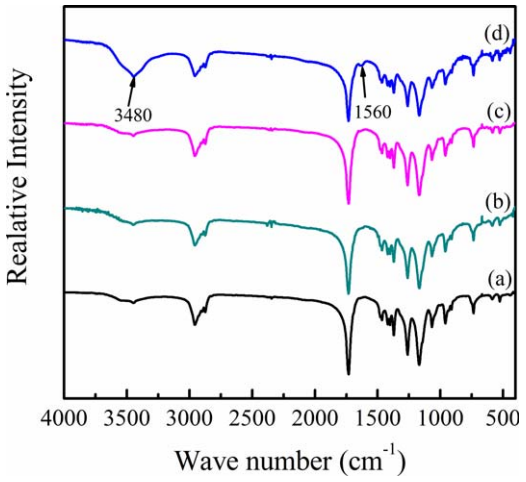

Figure 3. FTIR spectra of (a) PBA and (b) 0.1, (c) 0.2, and (d) 0.5 wt % PBA/m-LDH nanocomposites. [Color figure can be viewed in the online issue, which is available at wileyonlinelibrary.com.]

18 and 6 Å in length, respectively. The thickness of the hydroxide layer for LDH was calculated to be 4.8 Å. Those results suggest that the oleic acid and sorbitol intercalated into the LDH gallery could have possibly formed a bilayer structure in which the molecules of the organomodifier were assumed to tilt at a fixed angle to increase the interlayer spacing of LDH.

Figure 2 reveals the FTIR spectra of LDH and m-LDH. The lattice vibration peaks in the 500–800-cm^{-1} region were related to O—M—O and M—O groups, where M corresponds to Mg or Al.[16] In the FTIR data of LDH, an intense absorption band at 1635 cm^{-1} was due to the bending mode of water molecules in the interlayer gallery.[17] The characteristic peak at 1384 cm^{-1} was attributed to the asymmetric stretching vibrations of the interlayer nitrates. A broad adsorption band at about 3480 cm^{-1} was assigned to the O—H group stretching vibrations of hydroxide sheets in the LDH. The FTIR spectrum of m-LDH containing four extra absorption peaks at 1000, 1560, 2850, and 2920 cm^{-1} was extensively different from that of LDH. The characteristic peak at 1000 cm^{-1} was assigned to the stretching vibrations of the C—O group of the sorbitol. The absorption bands at 1560 cm^{-1} may have resulted from the asymmetric absorption of the COO^{-1} group of the oleic acid. Additionally, the absorption peaks at 2850 and 2920 cm^{-1} contributed to the symmetrical and asymmetric mode of the CH_3 and C=C—H groups of the oleic acid.[18,19] These results demonstrate that oleic acid and sorbitol were successfully intercalated into the interlayer spacing of the LDH.

Morphology and Thermal Properties of the PBA/m-LDH Nanocomposites

Figure 3 reveals the FTIR spectra of the PBA and PBA/m-LDH nanocomposites. From the FTIR data of PBA, an intense absorption band at 1735 cm^{-1} was assigned to the stretching vibrations of the C=O group of the ester.[20] The absorption bands at 1260 and 1175 cm^{-1} may have resulted from the asymmetric stretching of C—O—C and the stretching mode of the C—O group, respectively. The FTIR spectrum of the PBA/m-LDH nanocomposites, containing two extra absorption peaks at 1560 and 3480 cm^{-1}, was identical to that of m-LDH [Figure 2(b)]. These results demonstrate the presence of m-LDH in the nanocomposites. The interlayer spacing of the fabricated PBA/m-LDH nanocomposites determined with the XRD method is shown in Figure 4. All of the XRD scans of the PBA/m-LDH nanocomposites presented no diffraction peak at $2\theta = 1.4°$; this revealed that there was no regular periodicity in m-LDH. These results imply that the molecular chains of PBA could have been effectively inserted and well distributed into the interlayer of the m-LDHs. Although XRD is a powerful instrument for estimating the distribution of layered hydroxides in composites, TEM equipment can be used in a straightforward manner to visualize the exact intercalation or exfoliation degree of inorganic layered fillers in the polymer matrix. Figure 5 illustrates the TEM micrographs of the embedded and cut nanocomposite for the 0.5 wt % PBA/m-LDH nanocomposites. The TEM images of the PBA/m-LDH nanocomposites revealed that the original stacked structure of the LDH

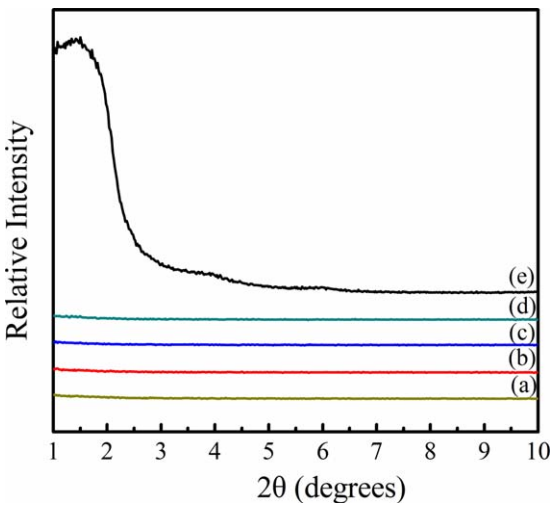

Figure 4. XRD data for the (a) PBA, (b) 0.1 wt % PBA/m-LDH, (c) 0.2 wt % PBA/m-LDH, (d) 0.5 wt % PBA/m-LDH, and (e) m-LDH. [Color figure can be viewed in the online issue, which is available at wileyonlinelibrary.com.]

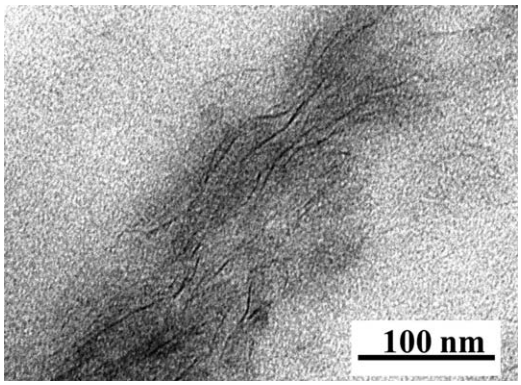

Figure 5. TEM micrographs obtained from embedded and cut 0.5 wt % PBA/m-LDH nanocomposites.

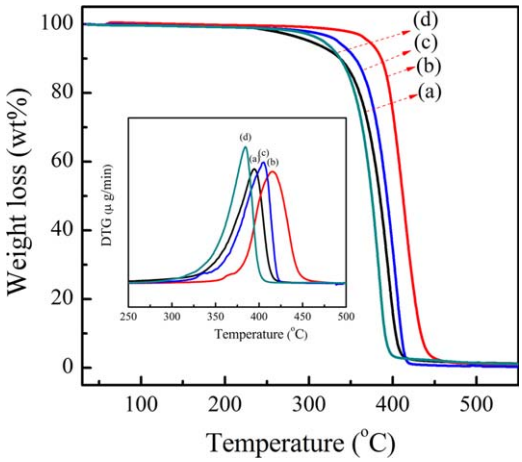

Figure 6. TGA patterns of the (a) neat PBA matrix and (b) 0.1, (c) 0.2, (d) 0.5 wt% PBA/m-LDH nanocomposites. The inset presents the differential thermal analyzer (DTA) curve for the related data. The differential thermal gravimetry (DTG) is obtained by the differentiation of TGA data vs. temperature. [Color figure can be viewed in the online issue, which is available at wileyonlinelibrary.com.]

galleries could be modified to form a disorderly morphology in the PBA matrix. From the previous XRD and TEM results, most of the hydroxide layers were found to be randomly exfoliated in the PBA matrix. Therefore, the preparation of the exfoliated PBA/m-LDH nanocomposites was performed successfully by the solution mixing process.

To study the influence of m-LDH on the thermal stability of the PBA matrix, TGA was used to examine the thermal degradation behavior of the PBA/m-LDH nanocomposites. The typical thermogravimetric profiles of weight loss for the PBA/m-LDH nanocomposites at a heating rate of 10°C/min are shown in Figure 6. All of the experimental results of the PBA/m-LDH nanocomposites exhibited a similar tendency, and the degradation temperatures obtained from these curves are summarized in Table I. All of the degradation temperatures, including the initial degradation temperature, temperature at 10% weight loss, temperature of the maximum degradation rate, and final degradation temperature, of the 0.1 and 0.2 wt % PBA/m-LDH composites were higher than those of the pure PBA matrix. For example, the temperature at 10% weight loss for neat PBA was 336.8°C, and surprisingly, it increased to 385.8°C with the loading of 0.1 wt % m-LDH. With the addition of more m-LDH to the PLLA matrix, the temperature at 10% weight loss decreased to 353.1 and 338.2°C for the 0.2 and 0.5 wt % PBA/m-LDH nanocomposites, respectively. These results reveal that the addition of organically modified LDH improved the thermal stability of the nanocomposites; this was similar to those reported in the literatures.[21–24] It was clearly observed that the presence of more m-LDH in PBA induced the worse thermal stability, in which the degradation temperature shifted obviously to lower temperatures. The degradation temperature of 0.1 wt % PBA/m-LDH was about 50°C higher than that of neat PBA, but it was slightly higher than that of PBA with a loading of 0.5 wt % m-LDH. These results imply that the thermal stability of the PBA/m-LDH nanocomposites significantly decreased with the m-LDH contents, and the amounts of Mg and Al increased. This phenomenon was attributed to the components of m-LDH, such as Mg and/or Al ions, which effectively catalyzed and accelerated the thermal degradation of PBA and reduced its thermal stability. Similar results have also been reported in previous publications.[25–27] Previous behaviors suggested that the thermal stability of PBA was strongly dominated by the presence of m-LDH, even with the addition of the highly thermally stable inorganic LDH. To investigate the effect of m-LDH on the crystal structure of PBA, the XRD method was used to determine the crystalline structure of the PBA and PBA/m-LDH nanocomposites. Figure 7 shows the XRD spectra of the neat PBA and PBA/m-LDH nanocomposites obtained at 40°C. Three diffraction peaks existed for neat PBA at 2θ values of 21.69, 22.41, and 24.08°, which corresponded to (010), (200), and (203), respectively, of the α-crystal form.[28,29] All of the data for the PBA/m-LDH nanocomposites were almost identical to those for PBA. These results suggest that the incorporation of m-LDH to PBA did not change the crystal arrangement of the PBA crystallized at 40°C.

Table I. Initial Degradation Temperature, Temperature at 10% Weight Loss, Temperature of the Maximum Degradation Rate, and Final Degradation Temperature of the PBA/m-LDH Composites

Sample	Initial degradation temperature (°C)	Temperature of 10% weight loss (°C)	Temperature of the maximum degradation rate (°C)	Final degradation temperature (°C)
PBA	289.2	336.8	383.0	404.0
0.1% PBA/m-LDH	354.7	385.8	414.0	452.1
0.2% PBA/m-LDH	321.3	353.1	402.1	416.9
0.5% PBA/m-LDH	288.8	338.2	383.9	400.0

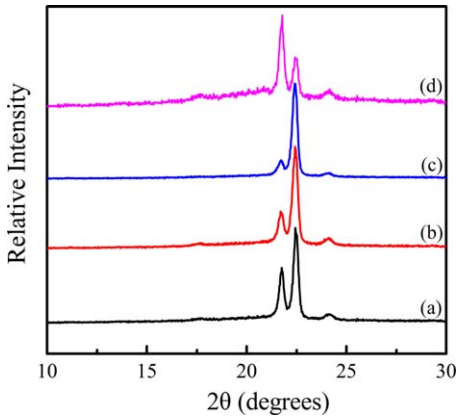

Figure 7. XRD data for the (a) PBA, (b) 0.1 wt % PBA/m-LDH, (c) 0.2 wt % PBA/m-LDH, and (d) 0.5 wt % PBA/m-LDH. [Color figure can be viewed in the online issue, which is available at wileyonlinelibrary.com.]

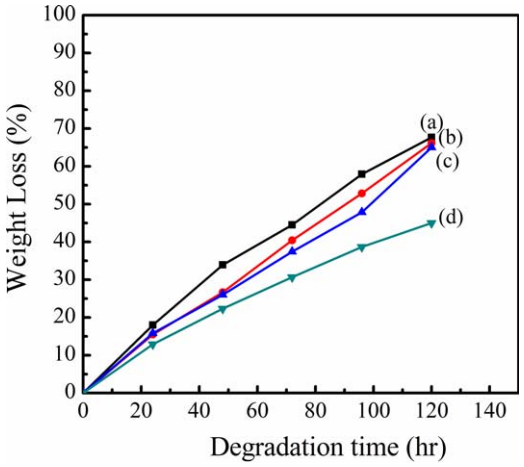

Figure 8. Dependence of the weight loss on the degradation time for the (a) PBA-based film and (b) 0.1, (c) 0.2, and (d) 0.5 wt % PBA/m-LDH nanocomposites. [Color figure can be viewed in the online issue, which is available at wileyonlinelibrary.com.]

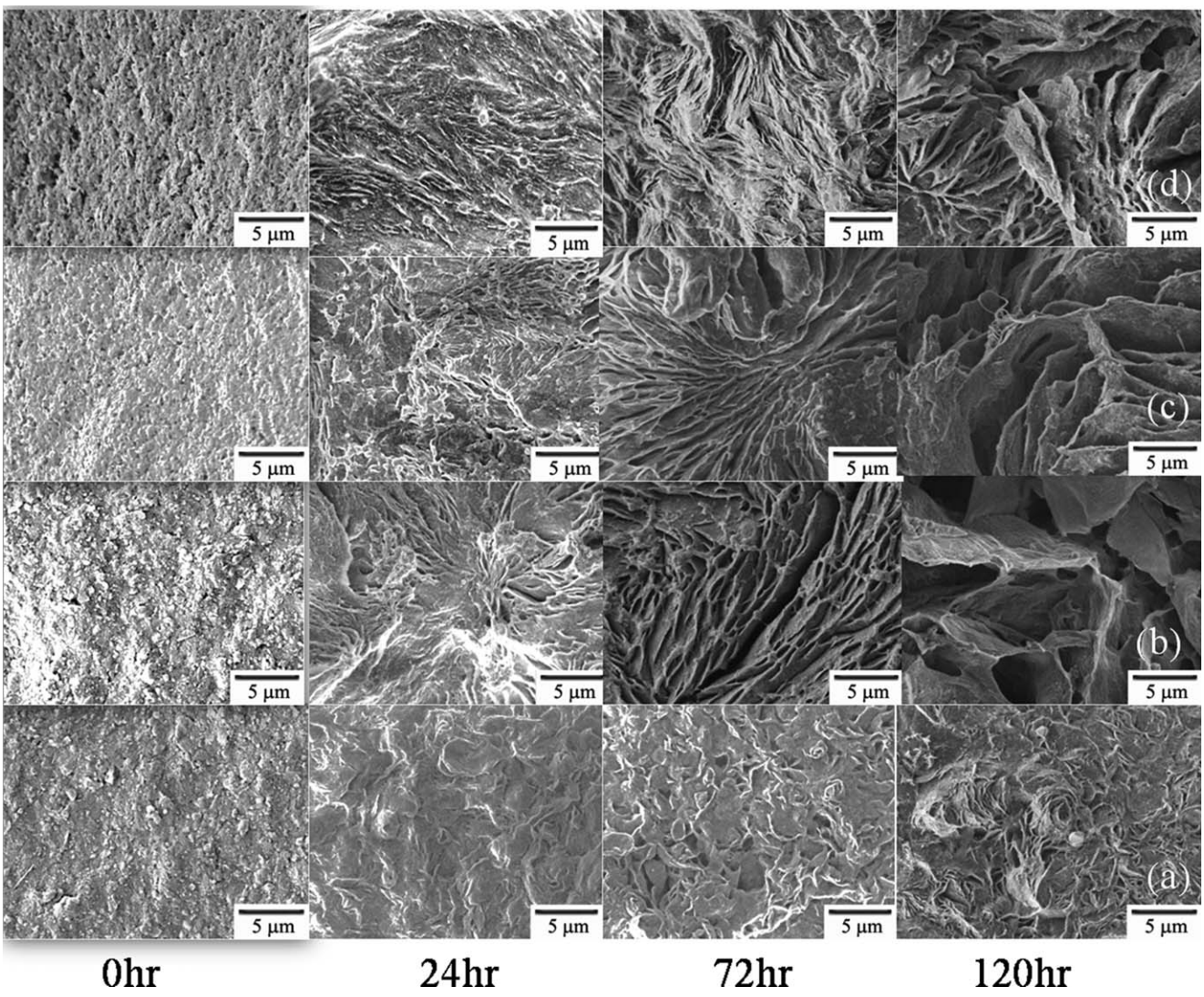

Figure 9. FESEM images of the microbially degraded (a) PBA and (b) 0.1, (c) 0.2, and (d) 0.5 wt % PBA/m-LDH nanocomposites.

Biodegradability of the PBA/m-LDH Nanocomposites

The microbial biodegradability of the PBA/m-LDH films is shown in Figure 8. The weight loss of the PBA/m-LDH film increased as the degradation time increased. Although the weight loss of the PBA film reached 67.7% after 120 h of incubation, the weight losses of the 0.1, 0.2, and 0.5 wt % PBA/m-LDH films were 66, 65.2, and 45%, respectively. Although the addition of 0.1 wt % m-LDH to PBA-based film significantly enhanced its thermal properties, the microbial biodegradability of the 0.1 wt % PBA/m-LDH film showed an insignificant difference. Because the addition of m-LDH in amounts of up to 0.5% in the PBA matrix slightly improved its thermal properties, the biodegradability revealed a significant difference. The biodegradability of a biodegradable polymer is a factor of the polymer's chemical composition, crystalline structure, degree of crystallinity, and steric conformation.[30–32] The chemical composition and crystalline structure were the same for all of the samples, whereas the degree of crystallinity for the PBA/m-LDH nanocomposites calculated from the XRD data was almost the same as that of the neat PBA matrix. Therefore, it was believed that the slower degradation rates of the 0.5 wt % PBA/m-LDH films were due to the increased degree of steric conformation with the loading of m-LDH to limit the motion of lipase from *P. fluorescens* and reduce the accessible attack spots for PBA depolymerase. Therefore, the degree of steric conformation was a vital factor in dealing with the degradation of the PBA/m-LDH nanocomposites.

The FESEM images of the degraded PBA/m-LDH films are shown in Figure 9. Before degradation, all of the films showed a similar surface morphology with a relative rough and porouslike character for the composite films. The surface morphology of the solvent-cast films could be affected by the presence of m-LDH. The surface conditions of the PBA/m-LDH film got more and more damaged within the incubation time course. When the incubation time was 24 h, the PBA/m-LDH composite residual films had a more damaged surface structure than PBA; this was consistent with the data presented in Figure 8. As shown by a comparison of the data of the neat PBA and PBA/m-LDH composite, the film made up of pure PBA had the most smooth surface, whereas the film made up of 0.5 wt % PBA/m-LDH had the roughest surface. After 72 h of degradation, oriented lines were observed on the PBA/m-LDH film surface; this was related to the α-form crystals.[33] With longer degradation time, more degradation occurred, and holes formed on the film surface. The size of holes for 0.1 wt % PBA/m-LDH was smaller than that of the 0.5 wt % PBA/m-LDH; this was also consistent with the data presented in Figure 8.

CONCLUSIONS

The XRD diffraction pattern demonstrated that the interlayer spacing of the LDH was 8.3 Å, where the interlayer spacing of m-LDH was 58.8 Å. These results suggest that not only the feasibility of the one-step coprecipitation for the synthesis of m-LDH but also that the intercalated oleic acid and sorbitol into the LDH gallery could further enlarge the interlayer spacing of LDH. Both the XRD and TEM results demonstrate that the majority of the hydroxide layers were exfoliated and randomly distributed in the PBA matrix. Therefore, the preparation of the exfoliated PBA/m-LDH nanocomposites was successful through the solution mixing process. With the loading of 0.1 wt % m-LDH, the thermal stability of the PBA/m-LDH nanocomposites was significantly improved. The addition of m-LDH in amounts up to 0.5% showed a considerable difference in terms of the biodegradability. After 120 h of degradation, the residual weight and surface morphology of the composite films was affected by the presence of m-LDH.

ACKNOWLEDGMENTS

The authors greatly appreciate the financial support provided by the National Science Council through project NSC102-2212-E-005-093.

REFERENCES

1. Sinha, R. S.; Bousmina, M. *Prog. Mater. Sci.* **2005**, *50*, 962.
2. Leung, V.; Ko, F. *Polym. Adv. Technol.* **2011**, *22*, 350.
3. Minke, R.; Blackwell, J. *J. Macromol. Sci. Phys.* **1979**, *16*, 407.
4. Minke, R.; Blackwell, *J. Macromol. Sci. Phys.* **1980**, *18*, 233.
5. Gan, Z.; Kuwabara, K.; Abe, H.; Iwata, T.; Doi, Y. *Biomacromolecules* **2004**, *5*, 371.
6. Zhao, Y.; Qiu, Z. *J. Nanosci. Nanotechnol.* **2012**, *12*, 4067.
7. Pavlidou, S.; Papaspyrides, C. D. *Prog. Polym. Sci.* **2008**, *33*, 1119.
8. Wang, D. Y.; Costa, F. R.; Vyalikh, A.; Leuteritz, A.; Scheler, U.; Jehnichen, D.; Wagenknecht, U.; Haussler, L.; Heinrich, G. *Chem. Mater.* **2009**, *21*, 4490.
9. O'Leary, S.; O'Hare, D.; Seeley, G. *Chem. Commun.* **2002**, 1506.
10. Choy, J. H.; Jung, J. S.; Oh, J. M.; Park, M.; Jeong, J.; Kang, Y. K. *Biomaterials* **2004**, *25*, 3059.
11. Yang, Q. Z.; Sun, D. J.; Zhang, C. G.; Wang, X. J.; Zhao, W. A. *Langmuir* **2003**, *19*, 5570.
12. Lin, J. J.; Juang, T. Y. *Polymer* **2004**, *45*, 7887.
13. Dagnon, K. L.; Chen, H. H.; Innocentini-Mei, L. H.; D'Souza, N. A. *Polym. Int.* **2009**, *58*, 133.
14. Millange, F.; Walton, R. I.; O'Hare, D. *J. Mater. Chem.* **2000**, *10*, 1713.
15. Chiang, M. F.; Wu, T. M. *Compos. Sci. Technol.* **2011**, *96*, 60.
16. Sanchez, J.; Tsuchii, A.; Tokiwa, Y. *Biotechnol. Lett.* **2000**, *22*, 849.
17. Tansengco, M. L.; Tokiwa, Y. *World J. Microbiol. Biotechnol.* **1998**, *14*, 133.
18. Calabia, B.; Tokiwa, Y. *Biotechnol. Lett.* **2004**, *26*, 15.
19. Hocking, P. J.; Marchessault, R. H.; Timmins, M. R.; Lenz, R. W.; Fuller, R. C. *Macromolecules* **1996**, *29*, 2472.
20. Yan, C.; Zhang, Y.; Hu, Y.; Ozaki, Y.; Shen, D.; Gan, Z.; Yan, S.; Takahashi, I. *J. Phys. Chem. B* **2008**, *112*, 3311.
21. Hsueh, H. B.; Chen, C. Y. *Polymer* **2003**, *44*, 1151.
22. Du, L. C.; Qu, B. J. *J. Mater. Chem.* **2006**, *16*, 1549.

23. Wang, G. A.; Wang, C. C.; Chen, C. Y. *Polym. Degrad. Stab.* **2006**, *91*, 2443.
24. Chem, W.; Feng, L.; Qu, B. *J. Chem. Mater.* **2004**, *16*, 368.
25. Chiang, M. F.; Chu, M. Z.; Wu, T. M. *Polym. Degrad. Stab.* **2011**, *96*, 60.
26. Nishida, H.; Fan, Y.; Mori, T.; Oyagi, N.; Shirai, Y.; Endo, T. *Ind. Eng. Chem. Res.* **2005**, *44*, 1433.
27. Motoyama, T.; Tsukegi, T.; Shirai, Y.; Nishida, H.; Endo, T. *Polym. Degrad. Stab.* **2007**, *92*, 1350.
28. Kai, W.; Zhu, B.; He, Y.; Inoue, Y. *J. Polym. Sci. Part B: Polym. Phys.* **2005**, *43*, 2340.
29. Dong, T.; Kai, W.; Inoue, Y. *Macromolecules* **2007**,*40*, 8285.
30. Tokiwa, Y.; Calabia, B.; Ugwu, C.; Aiba, S. *Int. J. Mol. Sci.* **2009**, *10*, 3722.
31. Jendrossek, D.; Schirmer, A.; Schlegel, H. G. *Appl. Microbiol. Biotechnol.* **1996**, *46*, 451.
32. Tokiwa, Y.; Calabia, B. *Biotechnol. Lett.* **2004**, *26*, 1181.
33. Zhao, L.; Gan, Z. *Polym. Degrad. Stab.* **2006**, *91*, 2429.